



DNA–DNA Interstrand Cross-Linking by *cis*-Diamminedichloroplatinum(II): N7(dG)-to-N7(dG) Cross-Linking at 5'-d(GC) in Synthetic Oligonucleotides

Huifang Huang, Jinsuk Woo, Stephen C. Alley and Paul B. Hopkins*

Department of Chemistry, University of Washington, Seattle, WA 98195, U.S.A.

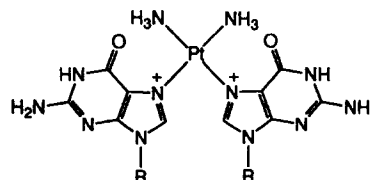
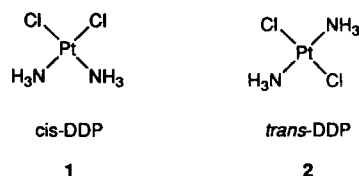
Abstract—The nucleotide sequence specificity of the DNA–DNA interstrand cross-linking reaction of *cis*-diamminedichloroplatinum(II) (*cis*-DDP) was studied in synthetic oligonucleotides. Of six self-complementary DNAs tested, only those containing the central sequence 5'-d(GC) formed appreciable interstrand cross-linked product, as assayed by denaturing polyacrylamide gel electrophoresis (DPAGE). The nucleotide connectivity of the interstrand cross-link was defined by sequence random oxidative fragmentation followed by DPAGE, revealing that dG residues on opposite strands at the sequence 5'-d(GC) were connected to one another. The covalent structure of the cross-link was established following hydrolysis of the phosphodiester backbone of a structurally homogeneous sample of a *cis*-DDP interstrand cross-linked DNA tetradecamer. HPLC analysis of the hydrolysate returned all of the deoxynucleoside residues from the starting DNA except for two deoxyguanosine residues. Also returned was diammine-bis-[N7-(2'-deoxyguanosyl)]platinum(II)²⁺, identified by a combination of spectroscopic methods, and comparison to a synthetic authentic sample. This study directly establishes that *cis*-DDP forms interstrand cross-links at the duplex sequence 5'-d(GC), linking deoxyguanosine residues on opposite strands at N7 through a bridging platinum atom. Computer simulation of the interstrand cross-linked product using molecular mechanics energy minimization and molecular dynamics revealed significant structural reorganization at the site of the cross-link including a *ca* 40° angle between the platinated guaninyl residues, which propagated to adjacent residues by base stacking to yield duplexes bent by some 30° toward the major groove.

Introduction

It is widely accepted that the cellular target of the antitumor drug *cis*-diamminedichloroplatinum(II) (cisplatin, *cis*-DDP, **1**) is DNA. Platinum–DNA adducts are capable of blocking DNA replication, which may account for their cytotoxicity.^{1–3} It is very well established that *cis*-DDP reacts predominantly at the N7 positions of purine bases, forming a variety of adducts. In random-sequence DNA, the majority of these lesions are intrastrand cross-links at the sequences 5'-d(GG) (*ca* 65%) and 5'-d(AG) (*ca* 25%), with the balance being a mixture of intrastrand cross-links at 5'-d(GXG) and interstrand cross-links.^{4,5} The intrastrand cross-links have been extensively structurally characterized; the interstrand cross-links have been the subject of far fewer investigations. The subject of this paper is the sequence preference with which *cis*-DDP forms interstrand cross-links in duplex DNA and the covalent structure and conformation of the resulting lesion.

It has not yet been possible to establish directly the relative contribution of the various lesions formed in DNA by *cis*-DDP toward its cytotoxic activity. While some studies have concluded that cytotoxicity is correlated with interstrand cross-linking, others have not.^{6,7} The argument that it is the intrastrand rather than interstrand lesion which is responsible for cytotoxicity⁸

is supported by the observation that *trans*-diamminedichloroplatinum(II) (*trans*-DDP, **2**), which does not form intrastrand cross-links and more efficiently forms interstrand cross-links,⁹ is considerably less cytotoxic. Furthermore, levels of platination with *cis*-DDP which were insufficient to form even a single interstrand cross-link destroyed the activity of DNA phage T7. For this reason, the intrastrand cross-links of *cis*-DDP have been the subject of extensive study.



3 R = 1-(β-D-2-deoxyribofuranosyl)

4 R = 1-(β-D-2-deoxyribofuranosyl)-5-monophosphate

A complete understanding of the therapeutic mechanism of action of *cis*-DDP will presumably require characterization chemically and biochemically of not only the active lesion(s), but the less active or inactive ones as well. We elucidate herein some structural features of the DNA interstrand cross-linking reaction of *cis*-DDP. Firstly, we show that *cis*-DDP preferentially forms interstrand cross-links in synthetic DNA duplexes which contain the nucleotide sequence 5'-d(GC), and that the efficiency of this reaction is a function of flanking sequence. These same conclusions were reached in an independent and methodologically distinct study¹⁰ published concurrently with our preliminary report.^{11,12} Subsequently, the structural distortions caused by this lesion¹³ and the mechanistic origin of the sequence selectivity have been probed.¹⁴ A more recent report using yet a third technique for the study of cross-linking sequence selectivity reached similar conclusions.¹⁵ Secondly, using a sequence-random fragmentation protocol, we demonstrate that this cross-link bridges deoxyguanosine residues on opposing strands at the 5'-d(GC) sequence. Thirdly, we have enzymatically digested the phosphodiester backbone of a homogeneous sample of a *cis*-DDP-interstrand cross-linked DNA and isolated the lesion responsible for the interstrand cross-link. This substance was characterized spectroscopically and by comparison to a chemically synthesized sample. The cross-link was shown to bridge dG residues at the 5'-d(GC) sequence with linkage through the two N7 positions of the dG residues. Computer simulation of the interstrand cross-linked product using molecular mechanics energy minimization and molecular dynamics revealed significant structural reorganization at the site of the cross-link, including a *ca* 40° angle between the platinated guaninyl residues, which propagated to adjacent residues by base stacking to yield duplexes bent by some 30° toward the major groove. This computational result complements related calculations and experiments reported by Sip *et al.*¹³ This knowledge will presumably contribute to the interpretation of experiments probing the biochemical consequences of this lesion (interaction with polymerases, repair enzymes, etc.).

Results

Sequence preference of *cis*-DDP cross-linking

To evaluate the sequence preferences of *cis*-DDP interstrand cross-linking reactions, a panel of six self-complementary DNAs was prepared which were identical in nucleotide sequence with the exception of the central four base pairs. The DNAs 5'-d[AATATAAT(N₄)ATTAT], (N₄=TCGA, TGCA, ACGT, AGCT, CCGG, GGCC), were 3'-end radiolabeled by Klenow filling using [α -³²P]dATP and treated with three equivalents of *cis*-DDP (60 mM sodium perchlorate, 3 mM potassium phosphate buffer, pH 7.6) at 37 °C for 14 h. The nucleic acid products were ethanol precipitated and analyzed by denaturing polyacrylamide gel

electrophoresis (DPAGE, Figure 1). All of the reaction mixtures returned a product (band I) identical in mobility to the starting single strands, a slightly lower mobility product (band II) which was presumed to be monoadducts and/or intrastrand cross-links, and a less mobile product (band III) which was believed to be interstrand cross-linked near the duplex termini. We have previously noted that the ends of synthetic duplexes are more reactive than centrally located sequences, and have proven this for the case of some cross-linking agents related to the mitomycin and pyrrolizidine alkaloid family.¹⁶ DNAs containing a 5'-d(GC) sequence (N₄=AGCT, TGCA, GGCC) produced one further product of even lower mobility (band IV), assumed in all cases (and proven below for one of the cases) to be an interstrand cross-linked product with the cross-link more centrally located in the duplex. The smallest nucleotide sequence common to these three DNAs and absent in the remaining three was the dinucleotide 5'-d(GC). The yields of these products (Table 1), determined by Cerenkov counting, revealed a pronounced preference for *cis*-DDP to cross-link DNAs which contain the sequence 5'-d(GC). The impact of flanking sequence was also evident, with a fivefold range of efficiency of cross-linking in the order AGCT > GGCC, TGCA.

Table 1. Yield of *cis*-DDP interstrand cross-linked DNA

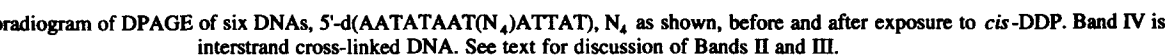
DNA (N ₄)	Yield (%)
ACGT	0.1
AGCT	6.7
TCGA	0.0
TGCA	1.3
CCGG	0.1
GGCC	1.8

Nucleotide connectivity of the interstrand cross-link

The nucleotide connectivity of the cross-linked product from the most efficiently cross-linked oligodeoxy-nucleotide N₄ = AGCT was analyzed at nucleotide resolution using Fe(II)/EDTA/hydrogen peroxide/ascorbic acid cleavage followed by DPAGE.¹⁷ This DNA was prepared separately in both 3'- and 5'-end radiolabeled form, cross-linked with *cis*-DDP, and the least mobile product on DPAGE was excised and eluted from the gel. Fragmentation of these products with the Fe(II)EDTA catalyst was followed by DPAGE separation of the resulting fragment mixtures (Fig. 2). In both radiolabeled forms, the largest radiolabeled fragment smaller in length than the full length single strand was due to cleavage at the lone G in the sequence (G10). This result is most consistent with the connectivity of the interstrand cross-link as dG-to-dG.

Covalent structure of the cross-link

In order to unequivocally determine the covalent



indicating the deoxyguanosine residues on both strands of the duplex were indeed the sites of attachment by *cis*-DDP. The HPLC trace also revealed that, in addition to returned nucleosides, there was a new strongly retained substance. If one assumed that the molar extinction coefficient at 260 nm of this new strongly retained substance was twice that of deoxyguanosine, it was estimated that 0.7 mol of this lesion was present per mole of hydrolyzed cross-linked DNA duplex. The proposal that this substance possessed the structure 3, in which the N7 positions of two dG residues are covalently linked to the platinum atom, is well preceded, but was formally established in this case by comparison to an authentic sample, the synthesis of which is described below.

Authentic samples of substances **3**^{18,19} and **4**^{20–22} were prepared by treatment of *cis*-DDP with 2'-deoxyguanosine

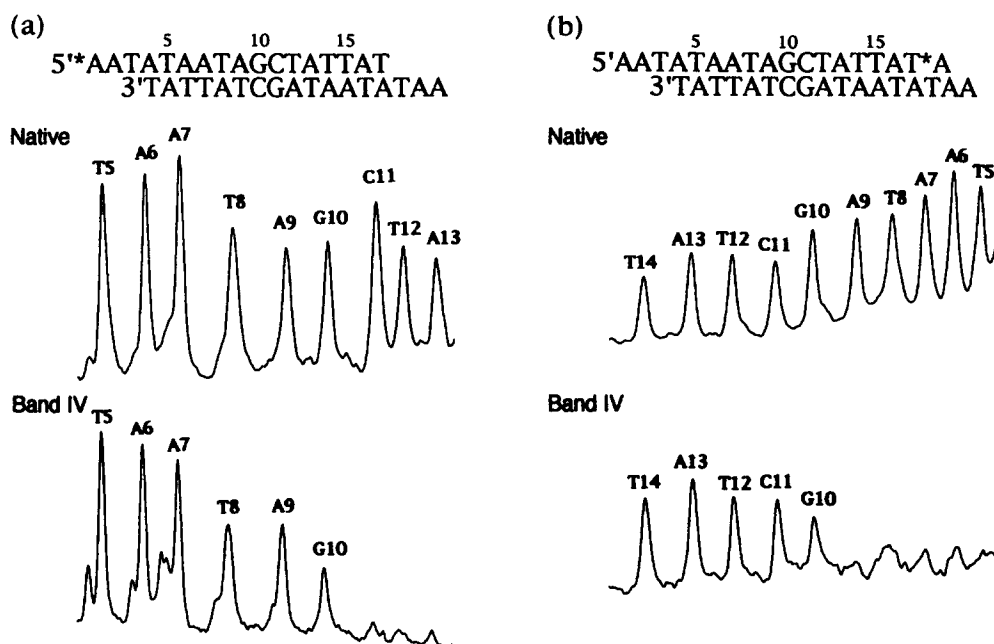


Figure 2. Partial fragmentation patterns for (a) 5'-end radiolabeled (* = ^{32}P) and (b) 3'-end radiolabeled band IV. Lettering indicates residue cleaved.

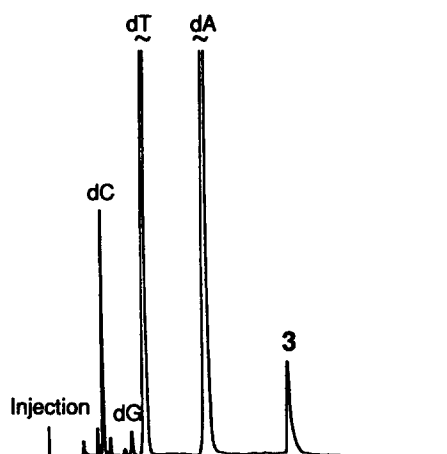


Figure 3. HPLC analysis of enzymatic hydrolysate of *cis*-DDP-interstrand cross-linked $[5'\text{-d(ATAATAGCTATTAT)}]_2$. Retention times increase to right; detection at 260 nm.

and 2'-deoxyguanosine-5'-monophosphate, respectively. The covalent structures of **3** and **4** prepared in this fashion have been unambiguously established previously, and we limited our characterization to observations which assured that we had isolated the same substances. Both **3** and **4** gave molecular ions ($M^{2+} - H^+$) in the electrospray ionization mass spectra consistent with the assigned structures, assuring the 2:1 molar ratio of nucleobase:platinum. Fragment ions for loss of one and two deoxyribosyl fragments assured in each case that the linkage to platinum was through the base rather than sugar. Ions containing platinum possessed the isotope distribution pattern characteristic of platinum. The ^1H NMR spectra of both **3** and **4** in D_2O at pH 6.5 each showed only a single set of resonances for the two deoxyribose residues, consistent with the chemical shift equivalence expected for the symmetrical structures **3** and **4**. Three observations

supported the well-established connection of platinum at N7. Firstly, the UV maxima for both **3** and **4** were red shifted by 6 nm relative to dG or dGMP, respectively. Secondly, the proton resonance for H8 was shifted downfield by 0.35 (**3**) and 0.5 (**4**) ppm relative to dG and dGMP, respectively. Thirdly, the H8 resonance in low field (90 MHz), but not high field (200 MHz or greater) ^1H NMR spectra of **3** possessed the broad satellite peaks with a *ca* 25 Hz spacing caused by ^{195}Pt - ^1H coupling²³ and in the integrated intensity predicted by the 34% abundance of ^{195}Pt . The chemical shift anisotropy of ^{195}Pt has been invoked to explain the extreme broadening of coupled ^1H resonances at high field.^{24,25} Finally, treatment of **4** with alkaline phosphatase returned **3** (HPLC, UV, and ^1H NMR analyses), assuring that **3** and **4** differed structurally only in the extent of phosphorylation.

Substance **3** prepared by enzymatic hydrolysis of interstrand cross-linked DNA was identical to substance **3** synthesized directly from *cis*-DDP and deoxyguanosine, as judged by three criteria: retention times in two HPLC systems, UV spectra, and electrospray ionization mass spectra.

Computational structures

Both the spacing and geometric orientation of the electron pairs of the two N7 atoms of the dG residues at the duplex B-DNA sequence 5'-d(GC) are incompatible with the spacing mandated by lesion **3**. Because of the high energetic cost of bond length and angle distortions relative to the costs of dihedral angle and stacking reorganization, it was expected that the structure of duplex DNA would be deformed at the site of the lesion. We relied upon molecular mechanics and dynamics simulations to provide a reasonable candidate

for the structure of this lesion in duplex DNA. This computation study complements that reported previously by Sip *et al.*, discussed below.¹³

A computer-generated model of the B-like duplex DNA [5'-d(GGGCCC)]₂ was modified by attachment centrally in the major groove of a *cis*-diammineplatinum(II) moiety at the N7 atoms of the central deoxyguanosine residues. Because of the inappropriate spacing of the N7 atoms in DNA, the bond length and angles of the N7-Pt-N7 bonds were substantially distorted from those observed in related crystal structures. This structure was energy minimized in the absence of solvent and counterions. Consistent with the high cost of bond length and angle deformation, in the minimized structure (Fig. 4, A and B) these values deviated only slightly from the optimal values. In achieving this, the deoxyguanosyl residues were shifted toward the center of the helix (Fig. 4A) and the planes occupied by the cross-linked purine bases were tilted some 40° relative to one another by the approach of the major groove 'edges' of these bases (Fig. 4B). Because this tilting diminishes favorable base stacking interactions, it was of interest to consider what features of the calculation drove this reorganization. Inspection of models revealed that the combination of the N7-Pt bond length, N7-Pt-N7 bond angles, and the dihedral angles about the N7-Pt bond rotors were especially important in this regard. To avoid biasing the calculated structure in favor of this tilting, the actual existence of which finds some support in experimental results,¹³ we had purposely parameterized rotation about the N7-Pt bonds to be without energetic cost. As such, the N7-Pt bond length and N7-Pt-N7 bond angles were implicated as the driving forces for this deformation.

To explore the possibility that the minimized structure might be a local minimum separated by some relatively minor structural modification from a lower energy and substantially structurally different conformational isomer, we performed a molecular dynamics simulation for 10 psec at 300 K. The five lowest energy structures along with five randomly chosen structures were then resubjected to energy minimization. The 10 resulting structures (Fig. 4C) spanned a range of 13.1 kcal mol⁻¹ in total energy, with the lowest energy structure being some 2.5 kcal mol⁻¹ in energy lower than the structure at the beginning of the dynamics run. The energies of the 'core' of the cross-linked structures, determined by deleting all but the cross-linked dinucleotide duplex (with hydroxyl termini), spanned a range of 3.5 kcal mol⁻¹, the lowest being 2.9 kcal mol⁻¹ lower than the starting core structure. The best superposition of these 10 new structures on the starting structure (Fig. 4C) revealed that despite the energetic changes noted, the global structural relationships of the platinum atom and its ligands were unchanged. That substantial structural change was possible under the conditions of the dynamics simulation was evident from the fact that some intermediate structures during the dynamics run possessed unpaired residues external to the core structure.

Although it was not a central emphasis of this work, the existence of computational and experimental support for a substantial bend in the helix axis of *cis*-DDP interstrand crosslinked DNA duplexes¹³ prompted us to inspect two of the calculated structures for bending. The structure after energy minimization and the lowest energy structure following dynamics and further minimization were bent by 25 and 35°, respectively, toward the major groove (Fig. 4D).

Discussion

We report herein that *cis*-DDP forms interstrand cross-links most efficiently in synthetic oligodeoxy-nucleotides which possess the sequence 5'-d(GC), and that this cross-link bridges the two N7 atoms of the deoxyguanosine residues on opposite strands at this sequence through a bridging platinum nucleus.

A panel of six self-complementary DNA duplexes incubated with *cis*-DDP and subsequently analyzed by DPAGE revealed that three of the six were interstrand cross-linked in strong preference to the others. The smallest sequence common to the DNAs which did interstrand cross-link but absent in those that did not was the sequence 5'-d(GC). The site of cross-linking was analyzed in one of these interstrand cross-linked DNAs at nucleotide resolution by the hydroxyl radical method,¹⁷ revealing the dG-to-dG connectivity. A closely related DNA containing one dG residue in each strand at a 5'-d(GC) sequence was cross-linked with *cis*-DDP and the interstrand cross-linked product isolated by DPAGE. Enzymatic digestion of the phosphodiester backbone returned essentially no dG (HPLC analysis), and in its place was found the lesion 3, which was identified by a combination of direct spectroscopic analysis (UV and electrospray ionization MS) and its identity with a synthetic sample of 3, prepared from *cis*-DDP and dG and identified by UV, MS, and ¹H NMR.

Eastman has extensively investigated the reactions of *cis*-DDP and a radiolabeled analog, *cis*-dichloro-(ethylenediamine)platinum(II) (*cis*-DEP), with deoxy-ribonucleosides and DNA. One study addressed the structure of the lesion responsible for interstrand cross-linking. A sample of platinated DNA enriched in *cis*-DEP-induced interstrand cross-links was obtained by exploiting the anomalously rapid renaturation of interstrand cross-linked DNA.²⁶ Enzymatic digestion of that sample returned what was identified based upon its HPLC retention time as the analog of 3 in which a single ethylenediamine replaces the two ammonia ligands on platinum. The author noted that this same lesion would have been returned from a 1,3-d(GNG) intrastrand cross-link. The possibility existed that the analog of 3 derived from interstrand cross-link enriched DNA may have come from intrastrand cross-links. Analogy to the results obtained herein with *cis*-DDP suggest that this was not likely to be the case, and the

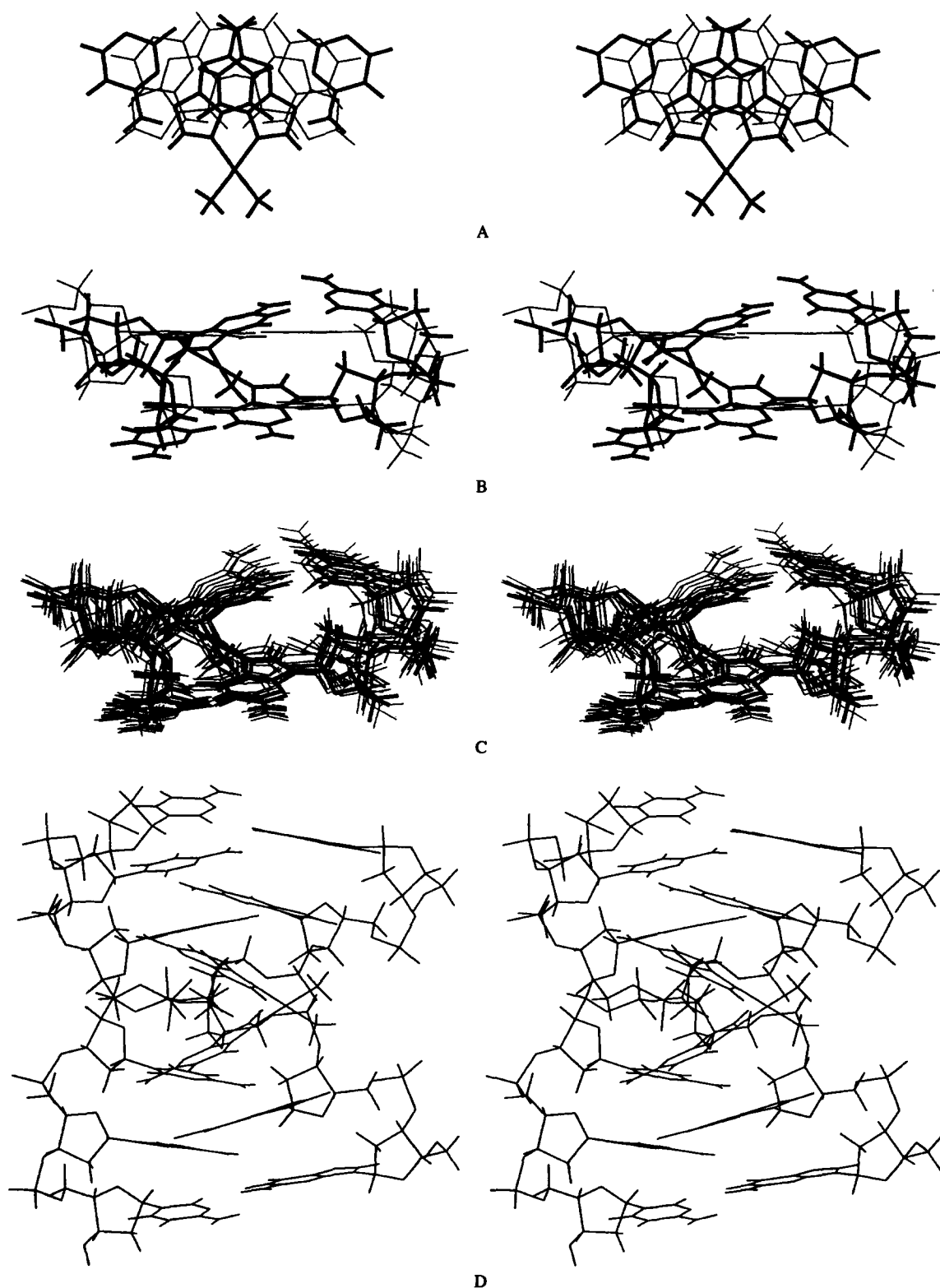


Figure 4. Stereoviews of cross-linked substructures (A–C) or structure (D) present in computer simulated *cis*-DDP interstrand cross-linked [5'-d(GGGCCC)]₂. (A) View down helix axis of energy minimized cross-linked base pairs (bold) superimposed on base pairs from B-DNA. (B) Same as A, except with the sugar-phosphate backbone included and viewed from the major groove. (C) Energy minimized cross-linked dinucleotide duplex (bold) viewed from major groove superimposed on 10 energy minimized structures taken from molecular dynamics simulation. (D) Lowest energy calculated structure after dynamics and energy minimization, viewed from the side.

central conclusions of Eastman appear to be valid. That study did not address the sequence-dependence of cross-linking.

Rahmouni and Leng⁹ demonstrated that *cis*-DDP interstrand cross-linked the synthetic oligonucleotides d[(CG)_n], n = 4 and 5, and concluded, based upon the

results of partial digestion of the phosphodiester backbone with nuclease P1, that the interstrand cross-links were between two guanine residues. Lemaire *et al.*,¹⁰ in a report contemporaneous with our preliminary report,¹¹ concluded on the basis of analysis of transcription stop sites in a *cis*-DDP-treated restriction fragment that interstrand cross-links were formed at 5'-d(GC) sequences. The deoxyguanosine residues involved in cross-linking were identified by their failure to react on sequential treatment with dimethylsulfate and piperidine. This observation also argues strongly for the involvement of N7 platination in interstrand cross-linking. Our own results are fully confirmatory of the central conclusions of Lemaire *et al.*¹⁰ Very recently another group¹⁵ has confirmed the substance of that report using a digestion/extension protocol, but there was no further characterization of the covalent structure.²⁷

We find through molecular mechanics and molecular dynamics calculations that the bridging of the two N7 atoms of the deoxyguanosine residues at the duplex sequence 5'-d(GC) by a single platinum atom and with *cis*-stereochemistry requires significant structural reorganization of B-DNA. Sip *et al.*¹³ independently recognized the likelihood of such distortions, and demonstrated bending of the helix axis experimentally by electrophoretic mobility studies of *cis*-DDP interstrand cross-linked oligonucleotide duplexes. Our calculations confirm the results of similar computations reported by Sip *et al.*,¹³ but are complementary in at least one respect. Whereas our focus was the local impact of a cross-link with the covalent structure 3, Sip *et al.* were interested in global bending of the helix axis caused by the cross-link. Molecular mechanics energy minimizations are poor at propagating the impact of a local stress as would be necessary for a B-DNA starting structure to become bent during the minimization. Presumably to overcome this hurdle, they built computer models of six interstrand cross-linked decamer duplex DNAs which were initially derived by kinking B-DNA by an amount ranging from 0 to 90°, and subsequently energy minimized these structures. The two lowest energy structures were derived from the bent starting structures and were themselves bent by 24 and 57°. We, in contrast, started with an unbent hexamer duplex in the B conformation, and used energy minimization and molecular dynamics to arrive at final structures. Our final structures are very similar to those of Sip *et al.*, particularly at the site of the cross-link, but also in that the lowest energy structures before and after molecular dynamics were bent by some 30°. This net bending is presumably the result of propagation through stacking of the *ca* 40° angle between the cross-linked guaninyl residues as constrained by their covalent linkage to platinum.

What is the origin of the preference for interstrand cross-linking at the sequence 5'-d(GC)? It is obvious from the sequence preferences of the intrastrand cross-linking reactions of *cis*-DDP and the interstrand cross-linking reactions of a number of other cross-linking

agents that proximity of the sites to be linked is an important feature. A total of some 90% of the lesions formed by *cis*-DDP are intrastrand cross-links which bridge N7 atoms on adjacent residues [5'-d(GG) and 5'-d(AG)]. 5'-d(PuPu) sequences possess the shortest distance between two N7 atoms in B DNA, and are thus presumably selected by *cis*-DDP to minimize distortion and thus destabilization of DNA. The 5'-d(GC) selectivity of the interstrand cross-linking reaction can then be understood to result from a combination of the inherent preference for platination of N7 of dG residues and the fact that this sequence also minimizes the N7-to-N7 distance which must be bridged, the 5'-d(PuPy) sequence having the shortest interstrand N7-to-N7 distance in B DNA. However, there remain subtle features of related reactions which are not well understood: the nitrogen mustard mechlorethamine likewise displays an inherent preference for N7 atoms of dG and possesses a relatively short tether. The prediction that it, too, would create interstrand cross-links at 5'-d(GC) sequences has been shown to be incorrect. Instead, N7 sites at 5'-d(GNC) are linked.²⁸ A trend which does appear to hold, however, is that cross-linking reactions in the major groove involving N7 will generally bridge purines with a 5'-offset (rather than 3'-offset), examples to date including *cis*-DDP, mechlorethamine,²⁸ DZQ,²⁹ diepoxybutane³⁰ and azinomycin.³¹

Experimental

Materials and general methods

Materials and their sources were as follows: DNA synthesis reagents, Applied Biosystems; phosphodiesterase I (*Crotalus adamanteus* venom), Pharmacia; alkaline phosphatase (calf intestinal) and P1 nuclease, Boehringer Mannheim; DNase I, Sigma; Sephadex G-25 superfine, Pharmacia; *cis*-Diamminedichloroplatinum (II) (*cis*-DDP), Aldrich. Water was purified on a Millipore Milli-Q deionizer. All other reagents were commercial and used as received. Unless otherwise specified, solutions were aqueous. Samples were concentrated on a Savant Speed Vac concentrator. Loading buffer was 90% aqueous deionized formamide containing 10 mM Tris/Tris-HCl (pH 7.5) and 1 mM Na₂EDTA. 1 × TBE buffer was 90 mM Tris-90 mM boric acid (pH 8.9) and 1.8 mM Na₂EDTA. Eluting Buffer was 500 mM NH₄OAc, 10 mM Mg(OAc)₂ and 1 mM Na₂EDTA. DNA radiolabeling buffer was 10 mM Tris/Tris-HCl (pH 7.5), 50 mM NaCl, 10 mM MgCl₂ and 1 mM DTT. DNA cross-linking reaction buffer 1 was 3 mM potassium phosphate (pH 7.6) and 60 mM NaClO₄. DNA cross-linking reaction buffer 2 was 2 mM potassium phosphate (pH 7.6) and 40 mM NaClO₄. Hydrolysis buffer 1 was 10 mM Tris/Tris-HCl (pH 7.5), 0.1 mM EDTA, and 4 mM MgCl₂. Hydrolysis buffer 2 was 50 mM Tris/Tris-HCl (pH 8.9) and 10 mM MgCl₂. *cis*-DDP stock solution was prepared by dissolving 4 mg of *cis*-DDP in 15 mL of water, and storing at 4 °C for 24 h prior to use. Autoradiography used Kodak XAR-5 film.

Cerenkov counting was performed on a Packard 2000 CA Tri Carb scintillation counter with a window setting 1 to 1000. UV spectra were measured on a Hewlett-Packard 8452A or a Perkin-Elmer Lambda 3A spectrophotometer. Nuclear magnetic resonance spectra (^1H NMR) were measured on a Bruker AC200 (200 MHz) or JEOL FX90 (90 MHz) spectrometer and, unless otherwise noted, are reported in parts per million downfield from external DSS (0.00 ppm). Electrospray ionization mass spectra (ESIMS) were measured on a Sciex Atmospheric Pressure Ionization triple quadrupole mass spectrometer. Operations, data display, and analysis were performed using Sciex' Tune (v. 2.3) and MacSpec (v. 3.21) software operating on a Macintosh IIfx. Except where otherwise noted, selected ions, diagnostic for the substance of interest, are reported. HPLC was performed on an Alltech, 5 mm, C18, 250 mm \times 4.6 mm Econosphere column using an SSI 200B/220B dual pump system with an SSI controller and SSI 500 UV/vis (output to a Linear 255/M recorder and an HP 3390A electronic integrator) detector. Solvent gradients were run at 1 mL min $^{-1}$. Gradient A: solvent A: 100 mM ammonium acetate (pH 7.0); solvent B: CH $_3$ CN; 7 min linear gradient from 94% A to 92% A, 13 min linear gradient to 60% A, 10 min linear gradient to 40% A, then 10 min linear gradient to initial conditions; Gradient B: The same program as gradient A except solvent A was 10 mM ammonium acetate (pH 7.0).

Preparation of DNA

Synthetic DNA was deprotected in concentrated aqueous ammonia at 55 °C for 16 h. Samples were dissolved in loading buffer, and purified by DPAGE [20% polyacrylamide (19:1 acrylamide:bis-acrylamide) and 8 M urea in 1 \times TBE buffer, 1.5 mm thick, 14 \times 16 cm]. Bands were visualized by UV shadowing, excised from the gel, crushed with a glass rod, and incubated at 25 °C for 14 h in eluting buffer. The resulting aqueous solution was desalted by passage through a Waters Sep-Pak C $_{18}$ cartridge previously washed with 10 mL of acetonitrile and 10 mL of water, followed by 10 mL of 10 mM aqueous ammonium acetate, 10 mL of water, and DNA eluted with 3 mL of 25% aqueous acetonitrile. DNA was recovered by concentration of the acetonitrile/water eluent to dryness. The DNA pellet was dissolved in water, quantified by UV and stored frozen at -20 °C until needed.

DNA (0.1 O.D., 0.36 nmol of duplex) was radiolabeled at the 3'-end by Klenow fragment and [α - ^{32}P]dATP. The DNA in 14 μL of water was treated with 2 μL of 10 \times DNA radiolabeling buffer, 3 μL (30 μCi) of [α - ^{32}P]dATP, and 1 μL (4 units) of Klenow fragment. The solution was tapped gently and allowed to stand at 25 °C for 20 min. Radiolabeling was stopped by ethanol precipitation: 10 μL of 3 M aqueous sodium acetate (pH 5.2) and 70 μL of water were added to radiolabeling solution above, followed by heating to 75 °C for 5 min. The resulting solution was treated with 0.7

mL of cold ethanol (-20 °C) and stored for 1 h at -20 °C. The precipitated DNA was pelleted by centrifugation, and the supernatant was discarded. The pellet was rinsed by suspension in 1 mL of 85% aqueous ethanol (-20 °C), centrifuged, and the supernatant decanted and discarded. The resulting pellet was dried in a vacuum centrifuge.

Reaction of cis-DDP with a panel of DNAs

The radiolabeled DNA prepared as above was dissolved in 1.2 μL (1.1 nmol) of *cis*-DDP stock solution and 4 μL of 10 \times DNA cross-linking reaction buffer 1, and diluted to a total volume of 40 μL with water. The solution was vortexed, then heated to 37 °C for 14 h. The resulting solution was ethanol precipitated and dried as described under 'Preparation of DNA,' except the step of 5 min heating at 75 °C was omitted. The DNA was dissolved in loading buffer and analyzed by DPAGE [25% polyacrylamide (19:1 acrylamide:bis-acrylamide) and 8 M urea in 1 \times TBE buffer, 0.35 mm thick, 34 \times 41 cm, using a 20-toothed comb].

Preparation of cross-linked DNA

In parallel, two 25 O.D. aliquots of 5'-[d(ATAATAGCTATTAT)] $_2$ were mixed with 100 μL of *cis*-DDP stock solution, 160 μL of 10 \times DNA cross-linking reaction buffer 2, and diluted to a total volume of 800 μL with water. The mixture was vortexed, centrifuged, and incubated at 25 °C for 18 h. The resulting sample was passed through a Waters Sep-Pak C $_{18}$ cartridge as described under 'Preparation of DNA.' DNA was recovered by concentration of the acetonitrile/water eluent to dryness. Pellet DNA was dissolved in 160 μL of a 1:1 mixture of water and loading buffer and purified by 25% DPAGE as described under 'Preparation of DNA'. Native and cross-linked DNA were visualized by UV shadowing and isolated from the gel by a crush and soak procedure: the band containing the cross-linked DNA was cut from the gel, crushed with a glass rod into fine particles, and incubated at 25 °C for 14 h in eluting buffer. The supernatant was removed and the gel incubated with fresh eluting buffer for an additional 1 h; this procedure was repeated once more. The supernatants were combined and passed through a Waters Sep-Pak C $_{18}$ cartridge as described before. UV readings of eluents were measured. Cross-linked DNA (4 O.D.) was recovered by concentration of the acetonitrile/water eluent (8% yield from starting native DNA).

Enzymatic hydrolysis of cross-linked DNA

Cross-linked DNA (4 O.D.) was hydrolyzed using 30 μL of hydrolysis buffer 1, 250 units of DNase 1, 30 units of P1 nuclease (freshly made by dissolving P1 nuclease pellet in water prior to use), 5 units of phosphodiesterase I, and 10 units of calf intestinal alkaline phosphatase (total volume 115 μL) at 37 °C for 14 h. HPLC analysis was carried out using gradient A. Peaks were identified by comparison of retention

times to those of authentic commercially available samples. Quantitation was based on the peak area ratios obtained from a standard, equimolar mixture prepared by weight of dC, dG, dT, and dA at 260 nm which were as follows: dC, 1.0; dG, 1.6; dT, 1.2; and dA, 1.9. Isolation of substance 3 from the hydrolysate of cross-linked DNA by HPLC was carried out using gradient B.

Chemical synthesis of 3

cis-DDP, 30 mg (0.1 mmol) and 58.4 mg of dG (0.205 mmol) were suspended in 22.5 mL of H₂O. The suspension was stirred for two days at 25 °C in the dark. The solution was then concentrated to 3–4 mL. A 1 mL aliquot of this concentrated solution was chromatographed over a column of Sephadex G-25 (superfine) (3.0 × 90 cm), and eluted with 50 mM aqueous NH₄HCO₃ (pH 8.5). Product 3 eluted at *ca* 760 mL and was detected by UV analysis of the fractions. The fractions containing 3 were pooled and concentrated on a rotary evaporator to a total volume of 1 mL. The concentrated sample was transferred to a microfuge tube. A small portion of this sample was retained for UV and ESIMS analysis; the remainder was further concentrated to dryness in a vacuum centrifuge. The dried sample was sequentially dissolved in D₂O and concentrated to dryness twice, then dissolved in 0.4 mL of 100 mM of sodium phosphate buffer (pH 6.5) in D₂O for ¹H NMR analysis. The sample for ESIMS was further purified by HPLC using gradient B. ESIMS (95 V inlet voltage, 4400 V needle voltage, 3 μL min⁻¹, sum of 40 scans): *m/z* 782 (M²⁺ – 2 H⁺ + Na⁺), 762 (M²⁺ – H⁺), 745 (M²⁺ – H⁺ – NH₃), 629 (M²⁺ – deoxyribosyl⁺ – NH₃), 513 (M²⁺ + H⁺ – 2 deoxyribosyl⁺), 496 (M²⁺ + H⁺ – 2 deoxyribosyl⁺ – NH₃), 379 (M²⁺ – deoxyribosyl⁺ – deoxyguanosine). ¹H NMR [200 MHz, D₂O, 100 mM sodium phosphate buffer (pH 6.5), external DSS]: δ 2.49 (2H, *ddd*, *J* = 5, 6, 14 Hz, 2' or 2''), 2.63 (2H, *ddd*, *J* = 6, 6, 14 Hz, 2' or 2''), 3.62 (2H, *dd*, *J* = 5, 13 Hz, 5' or 5''), 3.69 (2H, *dd*, *J* = 4, 13 Hz, 5' or 5''), 4.05 (2H, *ddd*, *J* = 4, 4, 5 Hz, 4'), 4.50 (2H, *ddd*, *J* = 4, 5, 6 Hz, 3'), 6.23 (2H, *dd*, *J* = 6, 6 Hz, 1'), 8.32 (2H, *s*, 8). UV spectrum: λ_{max} 260 nm (pH 7.0).

Chemical synthesis of 4

cis-DDP, 30 mg (0.1 mmol) and 71 mg of dGMP (0.205 mmol) were suspended in 22.5 mL of H₂O. The suspension was stirred at 50 °C for 3 h and then at 25 °C for 14 h in the dark. A 3 mL portion of this solution was chromatographed over a column of Sephadex G-25 (superfine) (1.6 × 53 cm), and eluted with 50 mM aqueous NH₄HCO₃ (pH 8.5). Substance 4 eluted at *ca* 90 mL, and was detected by UV analysis. This separation procedure was repeated once. The fractions containing 4 were pooled and concentrated on a rotary evaporator to a total volume of 1 mL. The concentrated sample was transferred to a microfuge tube. A small portion of the sample was retained for UV and ESIMS analysis, and the remainder was concentrated to dryness in a vacuum centrifuge. The dried sample was

sequentially dissolved in 0.4 mL D₂O and concentrated to dryness twice, then dissolved in 0.4 mL of 100 mM sodium phosphate buffer (pH 6.5) in D₂O for ¹H NMR analysis. ESIMS (95 V inlet voltage, 4400 V needle voltage, 3 μL min⁻¹, sum of 40 scans): *m/z* 922 (M + H⁺), 905 (M + H⁺ – NH₃), 709 (M + H⁺ – deoxyribosyl-5'-monophosphate – NH₃), 575 (M + H⁺ – deoxyguanosine-5'-monophosphate), 513 (M + H⁺ – 2 deoxyribosyl-5'-monophosphate – NH₃), 496 (M + H⁺ – deoxyguanosine-5'-monophosphate – HPO₃), 379 (M + H⁺ – deoxyribosyl-5'-monophosphate – deoxyguanosine-5'-monophosphate). ¹H NMR [200 MHz, 100 mM sodium phosphate buffer (pH 6.5), external DSS]: δ 2.54 (2H, *ddd*, *J* = 5, 6, 14 Hz, 2' or 2''), 2.66 (2H, *ddd*, *J* = 6, 6, 14 Hz, 2' or 2''), 3.86–4.08 (4H, *m*, 5' and 5''), 4.19 (2H, *ddd*, *J* = 4, 5, 5 Hz, 4'), 4.66 (2H, *ddd*, *J* = 4, 5, 6 Hz, 3'), 6.24 (2H, *dd*, *J* = 6, 6 Hz, 1'), 8.57 (2H, *s*, 8). UV spectrum: λ_{max} 260 nm (pH 7.0).

Preparation of 3 by enzymatic hydrolysis of 4

Substance 4 (80 O.D.) was hydrolyzed using 30 μL of hydrolysis buffer 2, and 30 units of calf intestinal alkaline phosphatase (total volume 330 μL) at 37 °C for 14 h. The product was purified as described under 'Chemical Synthesis of 3'. Substance 3 prepared by this method was shown to be indistinguishable from the direct product of *cis*-DDP reacting with dG using HPLC, UV and NMR analyses.

Computational studies

Computations were performed on a Silicon Graphics Iris Indigo XS-24 work station utilizing the Builder, Biopolymer, Discover (v. 2.9), and Analysis modules of Insight II (v. 2.2.0) (Biosym Technologies, San Diego, CA). Parameters for platinum and platinated guanines were generally as described previously. Bond length and bond angle parameters were from Ref. 32; atomic charges were from Ref. 33. With the following exception, all dihedral angles containing Pt were unconstrained. For Pt–N7–C5–C6, *E* = 12.2 kcal mol⁻¹ [1 + cos (2φ – 180°)] was used, as derived from Ref. 13. The starting structure was the B-like DNA [5'-d(GGGCCC)]₂ that had been platinated at the central 5'-d(GC) step, generated using the Builder module. The platinum atom was placed approximately half way between the platinated N7 atoms and in the major groove; the amino groups were oriented such that the N(H₃)–Pt–N(H₃) bond angle was 90°, and each amino group had one N(H₃)–Pt–N7 bond angle of 90°. Energy minimizations were performed with the AMBER force field, a distance-dependent dielectric of 4.0r in the absence of solvent and counter ions, a non-bonded cut-off of 12.0 Å, and no Morse or cross terms. Structures were minimized by the method of steepest descents for 200 iterations followed by the method of conjugate gradients until the maximum derivative for any atom was less than 0.01 kcal mol⁻¹ Å⁻¹ (requiring 1000 to 3000 iterations). In the molecular dynamics simulation, the minimized structure was equilibrated at 300 K for 0.2 ps, followed by 9.8 ps of molecular dynamics at

300 K. The step size was 1 fs, with snapshots taken every 100 fs. The five lowest energy structures (at 2.3, 3.5, 6.0, 9.0 and 9.9 ps) as well as five randomly chosen structures (at 1.2, 2.9, 4.9, 6.9 and 7.9 ps) were then energy minimized. Text references to the energy of 'core' structures refer to the energy of the structure resulting from the deletion of the four nucleotide base pairs not involved in cross-linking, and replacement of residual terminal phosphates or unfilled valences with hydrogens. Helix structures were in some cases evaluated using the program Newhelix 91, which was provided by Professor Richard Dickerson. The angle of bending of the helix axis for some structures was estimated as follows. Both ends of the calculated structures were extended with several turns of B-DNA, orienting the extensions so as to achieve best superposition of the heavy atoms of three nucleotide residue pairs in the computed structure with the corresponding atoms in the extending B-DNA. The bend angle was then either measured manually or by calculation of the angle between the top and bottom helix axes as determined using Newhelix 91.

Acknowledgments

This work was supported by the National Institutes of Health (GM45804 and GM32681). PBH was an Arthur C. Cope Scholar. HH acknowledges a fellowship from the Department of Chemistry, University of Washington. SCA was an NIH predoctoral fellow (GM08437). We thank Professor M. Cooke for providing the 90 MHz ¹H NMR spectrum of 3, Dr L. Zhu for technical assistance, Professor G. Drobny for valuable discussions, and the Department of Chemistry at UW for access to the computer molecular modeling facility. We thank Professor M. Leng for his comments on the manuscript. Phosphorimager was performed at the PhosphorImager Facility of the Markey Institute for Molecular Medicine. We thank Ms K. Bennett for assistance in the preparation of the manuscript.

References

1. Bruhn, S. L.; Toney, J. H.; Lippard, S. J. *Prog. Inorg. Chem.* **1990**, *38*, 477.
2. Heiger-Bernays, W. J.; Essigmann, J. M.; Lippard, S. J. *Biochemistry* **1990**, *29*, 8461.
3. Pinto, A. L.; Lippard, S. J. *Proc. Natl Acad. Sci. U.S.A.* **1985**, *82*, 4616.
4. Eastman, A. *Biochemistry* **1986**, *25*, 3912.
5. Fichtinger-Schepman, A. M. J.; van der Veer, J. L.; den Hartog, J. H. J.; Lohman, P. H. M.; Reedijk, J. *Biochemistry* **1985**, *24*, 707.
6. Roberts, J. J. In: *Molecular Mechanisms of Carcinogenic and Antitumor Activity*, pp. 463–489, Chagas, C.; Pullman, B., Eds; Pontifica Academia Scientiarum; Vatican City, 1987.
7. Roberts, J. J.; Knox, R. J.; Pera, M. F.; Friedlos, F.; Lydall, P. A. In: *Platinum and Other Metal Coordination Compounds in Cancer Chemotherapy*, pp.16–31, Nicolini, M. Ed.; Nijhoff; Boston, 1988.
8. Pinto, A. L.; Lippard, S. J. *Biochim. Biophys. Acta* **1985**, *780*, 167.
9. Rahmouni, A.; Leng, M. *Biochemistry* **1987**, *26*, 7229.
10. Lemaire, M.-A.; Schwartz, A.; Rahmouni, A. R.; Leng, M. *Proc. Natl Acad. Sci. U.S.A.* **1991**, *88*, 1982.
11. Hopkins, P. B.; Millard, J. T.; Woo, J.; Weidner, M. F.; Kirchner, J. J.; Sigurdsson, S. Th.; Raucher, S. *Tetrahedron* **1991**, *47*, 2475.
12. Woo, J. *DNA Cross-linking: The Minor Groove, The Major Groove and Between*, 1993, Ph.D. thesis, University of Washington.
13. Sip, M.; Schwartz, A.; Vovelle, F.; Ptak, M.; Leng, M. *Biochemistry* **1992**, *31*, 2508.
14. Payet, D.; Gaucheron, F.; Sip, M.; Leng, M. *Nucleic Acids Res.* **1993**, *21*, 5846.
15. Zou, Y.; Van Houten, B.; Farrell, N. *Biochemistry* **1994**, *33*, 5404.
16. Weidner, M. F.; Sigurdsson, S. Th.; Hopkins, P. B. *Biochemistry* **1990**, *29*, 9225.
17. Weidner, M. F.; Millard, J. T.; Hopkins, P. B. *J. Am. Chem. Soc.* **1989**, *111*, 9270.
18. Eastman, A. *Biochemistry* **1982**, *21*, 6732.
19. Johnson, N. P.; Mazard, A. M.; Escalier, J.; Macquet, J. P. *J. Am. Chem. Soc.* **1985**, *107*, 6376.
20. Marcelis, A. T. M.; van Kralingen, C. G.; Reedijk, J. *J. Inorg. Biochem.* **1980**, *13*, 213.
21. Polissiou, M.; Viet, M. T. P.; St.-Jacques, M.; Theophanides, T. *Inorg. Chim. Acta* **1985**, *107*, 203.
22. Fichtinger-Schepman, A. M. J.; van der Veer, J. L.; Lohman, P. H. M.; Reedijk, J. *J. Inorg. Biochem.* **1984**, *21*, 103.
23. Kong, P.-C.; Theophanides, T. *Inorg. Chem.* **1974**, *13*, 1167.
24. Lallemand, J.-Y.; Soulie, J.; Chottard, J.-C. *J. C. S. Chem. Comm.* **1980**, *10*, 436.
25. Ismail, I. M.; Kerrison, S. J. S.; Sadler, P. J. *Polyhedron* **1982**, *1*, 57.
26. Eastman, A. *Biochemistry* **1985**, *24*, 5027.
27. While this manuscript was in the final stages of preparation, Professor M. Leng provided to us further information concerning the study reported in Ref. 13. He reported that in the course of that study, they enzymatically degraded an interstrand cross-linked oligonucleotide and demonstrated the identity of the released platinum-containing nucleobase to an authentic sample using HPLC retention time. They noted a reduction in the quantity of released dG relative to the non-cross-linked oligonucleotides. The results reported in this manuscript are thus fully confirmatory of those from Professor Leng's laboratory. We thank Professor Leng for providing this information.
28. Rink, S. M.; Solomon, M. S.; Taylor, M. J.; Rajur, S. B.; McLaughlin, L. W.; Hopkins, P. B. *J. Am. Chem. Soc.* **1993**, *115*, 2551.

29. Alley, S. C.; Brameld, K. A.; Hopkins, P. B. *J. Am. Chem. Soc.* **1994**, *116*, 2734.
30. Millard, J. T.; White, M. M. *Biochemistry* **1993**, *32*, 2120.
31. Armstrong, R. W.; Salvetti, M. E.; Nguyen, M. *J. Am. Chem. Soc.* **1992**, *114*, 3144.
32. Mazeau, K.; Vovelle, F.; Rahmouni, A.; Leng, M.; Ptak, M. *Anti-Cancer Drug Design* **1989**, *4*, 63.
33. Herman, F.; Kozelka, J.; Stoven, V.; Guittet, E.; Girault, J. P.; Huynh-Dink, T.; Igolen, J.; Lallemand, J. Y.; Chottard, J. C. *Eur. J. BioChem.* **1990**, *194*, 119.

(Received in U.S.A. 3 October 1994; accepted 6 November 1994)